

segmental mobility and was hence observed to occur in the same temperature range as the glass transition process. This observation is consistent with the notion that most macroradicals generated on photolysis under vacuum ultimately decay via recombination with small radicals and also radical sites on side chains. Cross-linking is a much slower process and becomes an important pathway of radical deactivation only at a higher temperature or when photooxidation is carried out at 313 nm, causing photodissociation of main-chain hydroperoxy groups.

**Acknowledgment.** We thank Dr. D. Coulter for assistance in absorption measurements and A. Clayton in sample preparation. JPL Analytical Group support is also acknowledged. This paper is dedicated to Professor George Hammond for his pioneering research in the area of organic photochemistry.

## References and Notes

- (1) For Part 7, see: Gupta, M.; Gupta, A. *Polym. Photochem.*, accepted for publication.
- (2) Fox, R. B.; Isaacs, L. G.; Stokes, S.; Kagarise, R. E. *J. Polym. Sci., Part A-1* 1964, 2, 2085.
- (3) Phillips, D. *Photochemistry* 1976, 7, 505 and references therein.
- (4) Morimoto, A.; Takamitsu, I. *Prog. Org. Coat.* 1973, 1, 35.
- (5) Grassie, N.; Torrance, B. J. D.; Colford, J. G. *J. Polym. Sci., Part A-1* 1969, 7, 1425.
- (6) Fourie, J.; McGill, W. S. *Afr. J. Chem.* 1979, 32, 156.
- (7) McNeill, I. C.; Ackerman, L.; Gupta, S. N.; Zulfiquer, M.; Zulfiquer, S. *J. Polym. Sci., Polym. Chem. Ed.* 1977, 15, 2381.
- (8) Monahan, A. R. *J. Polym. Sci., Part A-1* 1966, 4 (10), 2381.
- (9) Monahan, A. R. *J. Polym. Sci., Part A-1* 1967, 5 (9), 2333.
- (10) Gupta, A.; Liang, R.; Tsay, F. D.; Moacanin, J. *Macromolecules* 1980, 13, 1696.
- (11) Rogers, C. E.; Simha, R.; Dickinson, H., private communication.
- (12) Cowell, G. W.; Pitts, J. N., Jr. *J. Am. Chem. Soc.* 1968, 90, 1106.
- (13) Gupta, A.; Yavrouian, A.; Di Stefano, S.; Merritt, C. D.; Scott, G. W. *Macromolecules* 1980, 13, 821.
- (14) Ausloos, P. *Can. J. Chem.* 1958, 36, 383. Wijnen, M. H. *J. Chem. Phys.* 1958, 28, 939. *Can. J. Chem.* 1958, 36, 69.
- (15) Rabek, J. F.; Skowronski, T. A.; Rånby, B. *Polymer* 1980, 21, 226.
- (16) Browing, H. L.; Hazel, Jr.; Ackermann, D.; Patton, H. W. *J. Polym. Sci., Part A-1* 1966, 4, 1433.
- (17) Szocs, F.; Rostasova, O. *J. Appl. Polym. Sci.* 1974, 18, 2529.
- (18) Geuskens, G.; David, C. *Makromol. Chem.* 1973, 165, 273.
- (19) Ng, H. C.; Guillet, J. E. *Macromolecules* 1978, 11, 929.

## Photoprocesses in Copolymers of Methacrylophenone with Methyl Methacrylate: Photodegradation and Intramolecular Energy Migration

Toomas Kilp\*

Radiation Laboratory, University of Notre Dame, Notre Dame, Indiana 46556

James E. Guillet

Department of Chemistry, University of Toronto, Toronto, Canada M5S 1A1

J. C. Galin and R. Roussel

Centre de Recherches sur les Macromolécules (CNRS), 67083 Strasbourg Cedex, France.

Received November 3, 1981

**ABSTRACT:** A series of poly(methyl methacrylate-co-methacrylophenone) copolymers were photolyzed in fluid solution with 313-nm radiation. Apparent quantum yields of degradation increased from 0.001 to 0.083 as the ketone content of the copolymers increased from 1.0 to 37.7 mol %. The magnitudes of these quantum yields are considerably lower than those previously reported for other methyl methacrylate-ketone copolymers. The depolarization of phosphorescence following excitation with plane-polarized light in 77 K solid solutions was measured as a function of copolymer composition. Results indicate that intramolecular energy transfer is a facile process in these systems. Migration of the excitation energy seems to be more dependent upon non-nearest-neighbor contacts between the ketone units than upon their presence in either dyad or triad sequences.

## Introduction

Previous studies of the photolysis of ketone copolymers characterized by an absence of hydrogen atoms  $\gamma$  to the carbonyl have yielded interesting and often contradictory results. For example, Amerik and Guillet<sup>1</sup> have found the quantum yield of main-chain scission in fluid solution to rise from a value of 0.04 in the homopolymer of methyl vinyl ketone to a value of about 0.20 in its copolymer with methyl methacrylate. Photolysis of the copolymer in the solid state at temperatures above its glass transition has been shown by Dan and Guillet<sup>2</sup> to result in quantum yields similar to those obtained in fluid solution. Kato and Yoneshige<sup>3</sup> have found that the copolymer of acrylophenone with  $\alpha$ -methylstyrene degrades much more slowly than does its copolymer with styrene. This behavior, which is attributable to a lack of abstractable  $\gamma$  hydrogens in the former case, was contradicted by their results of the photolysis of methyl vinyl ketone and acrylophenone co-

polymers with methyl methacrylate. The rapid degradation observed for these copolymers was unexpected in view of the lack of  $\gamma$ -hydrogen atoms. On the other hand, Lukac et al.<sup>4</sup> have found the quantum yield for main-chain scission of poly(acrylophenone) to be roughly halved when the ketone is copolymerized with methyl methacrylate.

Recently, Galin et al.<sup>5</sup> reported the first successful copolymerization of methyl methacrylate with methacrylophenone via a free radical mechanism. In view of the results cited above, it was felt that an investigation of some of the photoprocesses undergone by these copolymers would prove to be of interest.

## Experimental Section

Photolysis of the poly(methyl methacrylate-co-methacrylophenone), PMMA-MAP, copolymers in toluene solution at 32 °C was carried out with 313-nm radiation from a medium-pressure mercury arc lamp. A Schott narrow-band interference filter (JENA UV-PIL) was used to isolate the desired wavelength from

Table I  
Characteristics of PMMA-MAP Copolymers

polymer	MAP content <sup>a</sup>		method of polymerization	$\bar{M}_n^b$	$\Phi_s \pm 0.005^d$
	mol %	wt %			
PMMA-MAP-1	1.00	1.45	free radical	75 300	0.001, <sup>f</sup> 0.030 <sup>g</sup>
PMMA-MAP-2	2.90	4.18	modification <sup>e</sup>	46 700	
PMMA-MAP-3	3.15	4.53	free radical	32 000	0.022
PMMA-MAP-4	3.20	4.60	modification <sup>e</sup>	107 000	
PMMA-MAP-5	6.20	8.80	free radical	13 750	0.039
PMMA-MAP-6	8.80	12.35	free radical	17 400	0.055
PMMA-MAP-7	20.06	26.81	free radical	12 300	0.071
PMMA-MAP-8	37.70	46.91	free radical	5 200 <sup>c</sup>	0.083
PMAP	100.00	100.00	anionic	1 640 <sup>c</sup>	

<sup>a</sup> From UV absorbance in dioxane solution. <sup>b</sup> From membrane osmometry. <sup>c</sup> From vapor phase osmometry.

<sup>d</sup> Apparent quantum yield of chain scission. <sup>e</sup> Chemical modification of preformed PMMA polymer. <sup>f</sup> From final rate of degradation. <sup>g</sup> From initial rate of degradation.

the full lamp output. Degradation as a function of irradiation time was monitored by the technique of automatic viscometry.<sup>6</sup> Toluene was dried overnight with CaCl<sub>2</sub> and freshly distilled prior to use.

Emission spectra were obtained with a Perkin-Elmer Model MPF-2A fluorescence spectrometer as well as with an SLM 8000S photon-counting spectrofluorometer. The phosphorescence attachments used for low-temperature studies consisted of quartz Dewars into which 5-mm-o.d. quartz or Pyrex sample tubes could be fitted. The coolant in all cases was liquid nitrogen.

All spectra were recorded with 90° viewing of emission using polymer solutions that were  $(1-3) \times 10^{-3}$  M in ketone units.

The solvent used to form low-temperature glasses was in all cases  $\alpha$ -methyltetrahydrofuran ( $\alpha$ -MTHF) from Matheson Coleman and Bell. It was purified by refluxing over cuprous chloride for 3 h followed by distillation under a nitrogen atmosphere. No impurities were detectable in the absorption or emission spectra of the pure solvent. It was stored in a brown glass bottle under a blanket of nitrogen in order to inhibit impurity formation. Only freshly distilled solvent was used to make up solutions for emission studies. Any solution that was more than 2 or 3 days old was discarded and a fresh one was prepared for further work.

Degassing procedures were found to have no noticeable effect on the phosphorescence spectra in preliminary studies and were not carried out subsequently.

The shapes of the observed emission spectra were independent of whether precooling in an acetone-CO<sub>2</sub> bath or direct immersion into liquid nitrogen was used to produce the low-temperature glass. However, solutions were precooled prior to measurement of polarization values in order to produce glasses that were as strain-free as possible. Precooling invariably resulted in higher absolute values of the measured polarization.

The polarization  $p$  was determined as

$$p = \frac{I_{VV} - GI_{VH}}{I_{VV} + GI_{VH}} \quad (1)$$

and

$$G = I_{HV}/I_{HH} \quad (2)$$

where  $I$  is the intensity of the viewed emission, the first subscript indicates the position of the excitation polarizer, and the second subscript gives the position of the viewing polarizer. V and H refer to vertical and horizontal, respectively.

Instrumental depolarization is accounted for by  $G$ , a correction factor for the anisotropy introduced by any failure of the spectrometer diffraction gratings, quartz optics, and sample assembly to pass vertical and plane-polarized light with equal intensity.<sup>7</sup>

Polarizations measured as a function of the exciting wavelength were determined at the maximum of the 0-0 band of emission. Scattered light was minimized by keeping the spectrometer viewing slit as narrow as possible, usually 6 nm, and was rarely a problem. Loss of intensity due to narrow slit widths and the use of polarizers was partially compensated for by the use of a Pyrex Dewar and sample tube of 5 mm o.d., thereby increasing the effective path length of the solution. As absorption and emission occurred at  $\lambda > 300$  nm, the use of Pyrex posed no

problems. No inner filter effects were noticed due to the lack of overlap between absorption and emission spectra of the ketones investigated. The absolute error in the reported values is estimated at  $\pm 0.002$ .

The synthesis of the homopolymer of methacrylophenone (PMAP) and its copolymers with methyl methacrylate (PMMA-MAP) has been described by Galin et al.<sup>5</sup> The copolymers were of two types, the first being made by a normal free radical copolymerization of the two monomers. The second type was made by chemical modification of a preformed poly(methyl methacrylate) polymer using phenyllithium to displace the methoxy group in the ester.

## Results and Discussion

**Molecular Weight Changes.** The physical characteristics of the copolymers are listed in Table I as are the apparent quantum yields of chain scission  $\Phi_s$ . Only those polymers prepared by a free radical mechanism were photolyzed.

The polymers all exhibited a distinct absorption band ( $\epsilon = 153 \text{ M}^{-1} \text{ cm}^{-1}$  for PMAP) centered at 320 nm in  $\alpha$ -methyltetrahydrofuran solutions. An observed shift to 323 nm in toluene solutions is taken as being indicative of an  $n \rightarrow \pi^*$  transition. The ketone content of the copolymers was determined by their UV absorbance at 243 nm in dioxane solution using the value  $7830 \text{ M}^{-1} \text{ cm}^{-1}$  for the molar extinction coefficient for the homopolymer at this wavelength.

All of the copolymers with the exception of PMMA-MAP-1 exhibited sigmoidal scission-irradiation plots, characterized by a slow initial rate of degradation followed by a region of more rapid decreases in intrinsic viscosity. A leveling off at long exposure times occurred. This behavior can be attributed to greatly increased lifetimes due to a lack of abstractable  $\gamma$  hydrogens. This has been verified by Kiwi and Schnabel<sup>8</sup> for poly(methyl methacrylate-co-acrylophenone). In the absence of this mode of deactivation, bimolecular quenching by residual oxygen in the solution becomes significant. Degassing was accomplished only by an initial purge with a stream of nitrogen gas, as the freeze-thaw technique cannot be applied to solutions used in automatic viscometry.

Therefore, if the residual oxygen in our solutions is removed either by photoreaction or by further purging (as solution manipulation in the automatic viscometer is accomplished through the use of nitrogen gas under pressure), we might expect to see an initial upward curvature in the photolysis curves. The subsequent leveling off is then the well-known behavior exhibited by most polymer solutions undergoing photolysis.

Assuming classic inhibition kinetics are applicable, the uninhibited values of  $\Phi_s$  reported in Table I are determined from the apparent rate of increase in moles of bond scis-

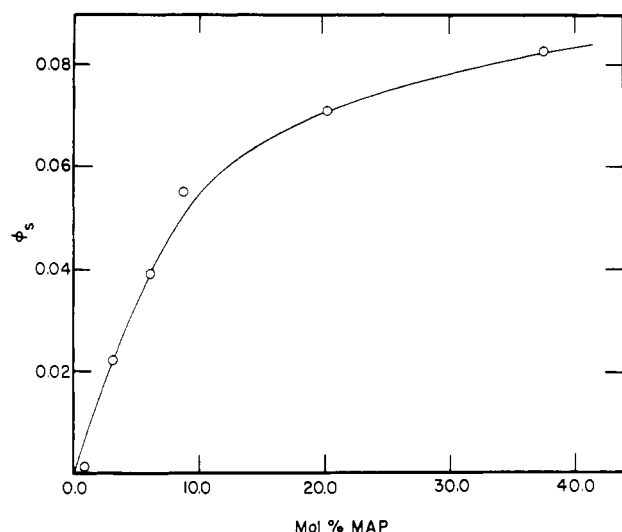
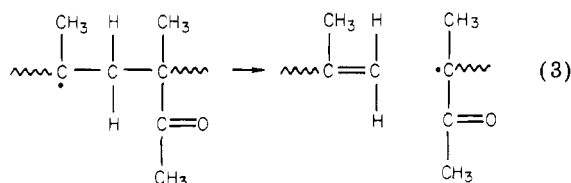


**Figure 1.** Dependence of  $\Phi_s$  on ketone content in PMMA-MAP copolymers.

sions with increasing absorbed radiation following the initial period of slow reaction. PMMA-MAP-1 was unusual insofar as it exhibited an exceptionally fast rate of photodegradation during the initial 10–15% of the photolysis followed by a much reduced rate thereafter. The two values of  $\Phi_s$  shown in Table I correspond to these two experimental regions. The variation of  $\Phi_s$  with ketone content is illustrated in Figure 1.

In the absence of  $\gamma$  hydrogens the classic Norrish type II reaction cannot occur. Amerik and Guillet<sup>1</sup> have proposed a seven-membered cyclic intermediate resulting in  $\delta$ -hydrogen abstraction in this case. Since  $\beta$ - or  $\delta$ -hydrogen abstraction involves torsionally strained rings of five and seven atoms, as opposed to the strain-free chair conformation in the normal type II process, this process is less efficient. Wagner et al.<sup>9</sup> have shown that in *n*-hexyl ketone the  $\gamma/\delta$ -hydrogen abstraction ratio is 20:1.

Shultz<sup>10</sup> has found a quantum yield of chain scission of 0.22 in poly(methyl isopropenyl ketone) using light of 253.7-nm wavelength. As this polymer is also characterized by a lack of  $\gamma$  hydrogens, a mechanism involving an initial type I cleavage producing a polymeric/small molecule radical pair was proposed. The former causes chain breaks via  $\beta$  scission:



That the Norrish type I reaction does not cause cleavage in other polymeric ketones of similar structure was attributed to the higher energy radiation ( $\lambda = 253.7$  nm) used in this experiment. If this mechanism is correct, then our  $\Phi_s$  values, which are much lower in comparison to those reported by Shultz, can be rationalized on the basis of the lower quantum yield for the type I process in PMMA-MAP. Wagner<sup>11</sup> and Lewis<sup>12</sup> have reported that the rate constants for type I cleavage of *tert*-alkyl phenyl ketones are only 1/100 as large as those of aliphatic ketones.

The  $\Phi_s$  values listed in Table I in all probability do not solely reflect chain scission. The extent of the photochemical reactions in our studies as well as those done by Shultz was monitored through changes in the intrinsic viscosity  $[\eta]$ . The magnitude of  $[\eta]$  is dependent upon the

hydrodynamic volume of the polymer chains and can decrease as a result of either molecular weight reduction or intramolecular cross-linking. The latter results in decreased molecular mobility and reduces the hydrodynamic volume. The formation of cross-links is quite likely in this case, as intramolecular hydrogen abstraction produces polymeric radicals whose ability to diffuse apart is greatly reduced in comparison to smaller molecular weight species. A similar mechanism has been proposed by Geuskens et al.<sup>14</sup> to account for the reduction of the intrinsic viscosity of dilute poly(vinylbenzophenone) solutions upon irradiation. This hypothesis is currently being examined in more detail by the use of laser flash photolysis techniques.

The initial increase in  $\Phi_s$  values as shown in Figure 1 may then reflect the increasing probability of formation of intramolecular cross-links as the ketone content of the copolymers increases. The changes in  $\bar{M}_n$  with percent ketone as shown in Table I may also play a part as the trend correlates with the generally observed decrease in polymeric coil densities with an increase in molecular weight. The subsequent leveling off probably reflects a decreased molecular weight dependency for changes in  $[\eta]$  with cross-linking. Regardless, the values of  $\Phi_s$  listed in Table I represent apparent quantum yields of degradation roughly an order of magnitude less than those reported previously<sup>1-3</sup> for other methyl methacrylate-ketone copolymers.

**Emission Studies.** The use of plane-polarized light in the investigation of polymeric systems has been common practice for many years. Depolarization of the observed emission can result either from molecular motions that occur on the same time scale as the lifetimes of the emitting states or from energy migration. Weber<sup>15</sup> has discussed the implications of both mechanisms.

In rigid media, where large-scale molecular motions may be taken to be negligible, depolarization due to energy migration becomes possible. Schneider<sup>16</sup> was the first to study this phenomenon in a synthetic polymer by measuring the fluorescence depolarization of poly(vinylcarbazole) in solid solutions. More recently, Geuskens et al.<sup>17,18</sup> have reported on the efficiency of energy migration as a function of composition for a variety of copolymers in both frozen glasses and films. Several treatments of concentration depolarization in solutions of small molecules have been developed and applied with varying degrees of success. Common to all of these theories is the assumption of a random spatial distribution and orientation of the chromophores. Of the various theories put forth, three are more commonly encountered in the literature. They are the Jablonski,<sup>19</sup> the Förster-Ore,<sup>20</sup> and the Weber<sup>21</sup> models. All three predict a linear relationship between  $1/p$  and the fluorescent solute concentration at low values of the latter.

Measurements of the phosphorescence polarization  $p$  of the PMMA-MAP copolymers as a function of excitation wavelength and polymer composition are listed in Table II. Shown as well are the results from the small-molecule model compounds acetophenone and isobutyrophenone.

Several interesting trends are immediately apparent. First, the extent of phosphorescence depolarization increases with ketone content in the copolymer, and emission from the homopolymer PMAP is completely depolarized within experimental error. For a given copolymer composition there is a slight, but noticeable, increase in  $p$  with increasing wavelength of excitation. This is not seen with the small molecules acetophenone and isobutyrophenone.

The similarity in the values obtained for PMMA-MAP-3 (3.15 mol % ketone) and PMMA-MAP-4 (3.2 mol

Table II  
Phosphorescence Polarization<sup>a,b</sup> of PMMA-MAP Copolymers

$\lambda_{\text{excite}}$ , nm	mol % ketone										aceto- isobutyro- phenone phenone	
	1.00	2.90	3.15	3.20	6.20	8.80	20.06	37.70	100.0			
325	0.059	0.053	0.042	0.031	0.034	0.026	0.016	0.010	-0.002	0.078	0.074	
330	0.066	0.055	0.047	0.048	0.041	0.032	0.020	0.011	0.002	0.068	0.070	
335	0.066	0.058	0.048	0.052	0.040	0.033	0.019	0.012	0.001	0.076	0.079	
340	0.068	0.049	0.050	0.045	0.040	0.031	0.017	0.010	0.006	0.077	0.072	
345	0.062	0.044	0.050	0.054	0.038	0.031	0.019	0.010	0.000	0.074	0.075	
350	0.064	0.052	0.047	0.050	0.041	0.032	0.022	0.012	0.000	0.075	0.071	

<sup>a</sup> For 0-0 band of emission. <sup>b</sup> Estimated error  $\pm 0.002$ .

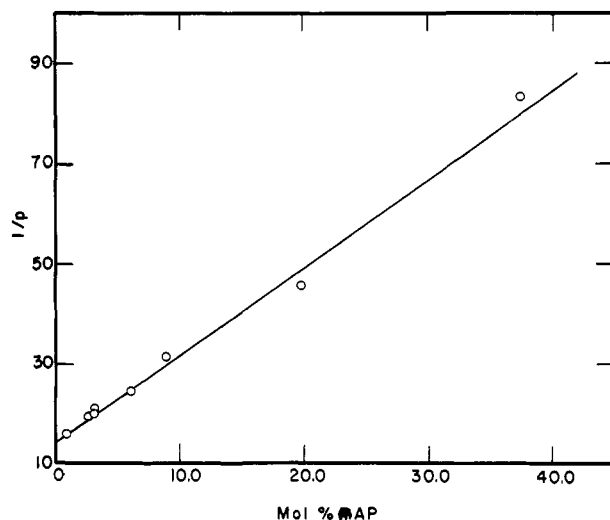


Figure 2. Phosphorescence polarization as a function of PMMA-MAP composition.  $\lambda_{\text{excite}}$  was 350 nm and all solutions were  $(1-3) \times 10^{-3}$  M in ketone units.

% ketone) is also interesting in view of the differences in their synthesis and number-average molecular weights.

Figure 2 shows the reciprocal of the phosphorescence polarization plotted as a function of copolymer composition. The excitation wavelength was 350 nm in this case. For copolymer compositions of up to 37.7 mol % ketone, excellent linearity was observed regardless of excitation wavelength. This behavior is in good accord with theory. Extrapolation to 0 mol % MAP yields an ordinate intercept of 14, which corresponds to a polarization of 0.071 for a completely isolated ketone unit in an otherwise pure, infinitely long poly(methyl methacrylate) chain. This is in good agreement with the values of 0.075 and 0.071 obtained for the small-molecule model compounds acetophenone and isobutyrophenone.

However, since the phosphorescence of the homopolymer is completely depolarized, departure from linearity must occur at some higher copolymer composition. In the case of poly(styrene-co-vinylbenzophenone), Geuskens et al.<sup>17</sup> found this behavior for copolymers containing more than 50-65% of the aromatic carbonyl. They attributed this to an increase in the efficiency of energy migration.

Energy migration in a polymeric system can occur as a result of both nearest- and non-nearest-neighbor interactions. The latter are important when different segments of the polymer coil approach sufficiently near to each other to allow interactions of the chromophores contained within them. The extent to which these occur will depend not only on the overall composition of the polymer and the sequence distribution of the comonomers but on the degree of expansion of the polymer coil.

The sequence distributions in the PMMA-MAP copolymers prepared by free radical polymerization have

Table III  
Sequence Distribution of PMMA-MAP Copolymers<sup>a</sup>

polymer	mol % MAP	$F_{ABA}$	$F_{BBA}$	$F_{BBB}$	$p \pm$ 0.002 <sup>b</sup>
PMMA-MAP-1	1.00	0.9869	0.0131	0.0000	0.068
PMMA-MAP-3	3.15	0.9667	0.0633	0.0003	0.050
PMMA-MAP-5	6.20	0.9252	0.0733	0.0015	0.040
PMMA-MAP-6	8.80	0.9043	0.0933	0.0024	0.031
PMMA-MAP-7	20.06	0.7511	0.2311	0.0178	0.017
PMMA-MAP-8	37.70	0.5211	0.4015	0.0776	0.010
PMAP	100.00	0.0000	0.0000	1.0000	0.006

<sup>a</sup> A and B refer to MMA and MAP units, respectively.

<sup>b</sup> Polarization of 0-0 band following 340-nm excitation.

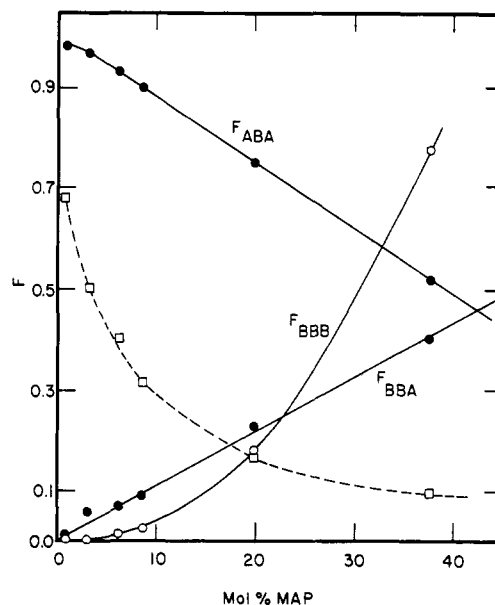


Figure 3. Correlation of phosphorescence depolarization with sequence distributions of PMMA-MAP copolymers. Note: values for  $F_{BBB}$  are  $\times 10$ ; (---) phosphorescence polarization  $\times 10$  for  $\lambda_{\text{excite}} = 340$  nm.

been calculated<sup>5</sup> by assuming that copolymerization occurs according to the penultimate model as defined by Harwood.<sup>22</sup> Galin<sup>5</sup> has determined the values of the reactivity ratios  $r_{AA}$ ,  $r_{BA}$ ,  $r_{BB}$ , and  $r_{AB}$  to be 1.77, 2.30, 0.058, and 0.325, respectively, where A refers to an MMA monomer and B to the MAP unit. Table III lists the resultant mole fractions  $F$  of MAP dyads (BBA) and triads (BBB) as well as the isolated MAP (ABA) content of the copolymers as a function of their overall composition.

It can be seen that as the percent MAP increases, the dyad and triad contents in the copolymers do likewise. Figure 3 illustrates the trends in sequence distribution as listed in Table III. Also shown is the decrease in phosphorescence polarization as a function of ketone content for excitation at 340 nm. It should be noted that these values as well as those for  $F_{BBB}$  have been multiplied by

a factor of 10 in order to show them on the same plot as  $F_{ABA}$  and  $F_{BBA}$ .

Phosphorescence depolarization does not directly correlate with changes in dyad, triad, or isolated ketone unit content, taken individually. The largest decreases in  $p$  occur from 0 to 8% MAP, a region where both dyad and triad contents change only very slowly. From Table II we can see that PMMA-MAP-3 and PMMA-MAP-4 (3.15 and 3.20% MAP, respectively) have very similar polarization values. The latter, prepared by chemical modification of a preformed PMMA polymer, may contain a higher percentage of isolated ketone units than the former. The probability of having substitution occurring on adjacent ester groups in the PMMA chain is very low when the modification is kept to low conversions, as was the case here. Depolarization in this region must therefore reflect primarily non-nearest-neighbor effects although the increase in ketone content alone does not seem to be sufficient to explain the large drop in  $p$ . Increases in dyad and triad contents almost certainly play a part here.

Above 20% MAP, BBA and BBB interactions probably make the major contribution to the observed depolarization. However, the  $p$  values in this range of composition are sufficiently low that the magnitude of the experimental error precludes a reliable estimate of their relative importance.

The strict application of any of the current models for concentration depolarization to the emission from polymeric chromophores is not possible. For example, Weber<sup>21</sup> considered the situation wherein an emission oscillator is subjected to a series of small changes in its orientation, each characterized by an angle  $\theta$  and occurring in mean number  $\langle n \rangle$  during the lifetime of the excited state, and derived the following relationship:

$$(1/p - 1/3) = (1/p_0 - 1/3)[1 + (3/2)\langle \sin^2 \theta \rangle \langle n \rangle] \quad (4)$$

where  $p_0$  is the emission polarization at infinite dilution. The values of  $\langle \sin^2 \theta \rangle$  and  $\langle n \rangle$  are dependent upon the mechanism of energy transfer and are functions of the angular  $\nu(\theta)$  and radial  $\nu(r)$  probabilities of energy transfer. The radial dependence of energy transfer by an exchange mechanism has been described by Inokuti and Hirayama<sup>23</sup> while some controversy remains as to the magnitude of the angular dependence.<sup>24</sup> However, all current expressions for  $\nu(r)$  and  $\nu(\theta)$  are derived with the assumption that the chromophores are isotropically distributed throughout the solution and are randomly oriented with respect to each other. These requirements are clearly not met in dilute polymer solutions where the effective concentrations of the bound chromophores are much higher than those calculated on the basis of their isotropic distribution throughout the medium. Furthermore, steric interactions within the polymer chain will result in preferred local conformations, thereby affecting the assumption of a random mutual orientation of the bound chromophores. Analysis of our data on the basis of expressions such as that shown in eq 4 is therefore not possible at this time.

The phosphorescence polarization of the PMMA-MAP copolymers as a function of the excitation wavelength is shown in Figure 4. A definite trend to lower  $p$  values with shorter excitation wavelengths is apparent, only the line corresponding to 340 nm failing to obey the general behavior. These variations have been previously noted in small molecules by Dörr.<sup>25</sup>

The wavelengths used in our studies correspond to excitation of the  $n \rightarrow \pi^*$  transition, which is forbidden on the basis of symmetry. That it occurs at all is due to "intensity borrowing" through vibronic coupling to a higher allowed state, created by a vibration of a suitable sym-

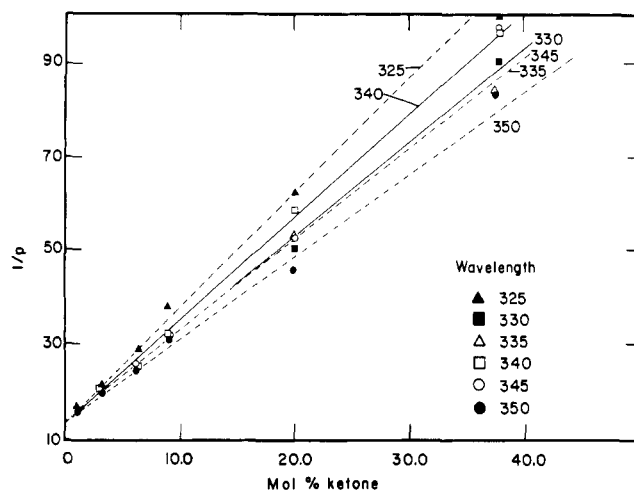


Figure 4. Phosphorescence polarization of PMMA-MAP copolymers as a function of copolymer composition and excitation wavelength.

metry.<sup>26</sup> The assumption that is often made in phosphorescence measurements, then, is that the magnitude of the observed polarization is independent of the nature of the vibronic coupling in the excitation step. From Table II we see that this is a good approximation for the small molecules acetophenone and isobutyrophenone but not necessarily for the polymeric ketones. In the latter case, the carbonyl groups undergo mutual interactions to a larger extent than do those in dilute small-molecule solutions as a consequence of their bonding to the polymer backbone.

Variations in the wavelength of irradiation then can lead to changes in the magnitude of the observed phosphorescence polarization as a result of the excitation of different vibrational levels, characterized by different vibronic interactions. However, as has been pointed out by Geuskens et al.,<sup>17</sup> this would still result in plots with equal slopes but varying intercepts when the data are analyzed in accordance with the theoretical models mentioned previously. The increase in slope might then be due to a change in the vibronic interactions in the MAP units themselves as the copolymer composition changes. Such behavior should be noticeable by changes in either the absorption or emission spectra as a function of ketone content.

## Conclusions

Apparent quantum yields of chain scission for PMMA-MAP copolymers are roughly an order of magnitude less than those reported previously<sup>1-3</sup> for other methyl methacrylate ketone copolymers. The decreases in  $[\eta]$  are probably due mainly to  $\beta$  scission of type I radicals but may also be partly attributable to a decrease in hydrodynamic volume as a consequence of intramolecular cross-linking.

The rapid depolarization of the phosphorescence of the polymeric carbonyls in dilute solid solutions at 77 K as the mole fraction of ketone monomer in the copolymers increases is indicative of a very facile intramolecular triplet energy transfer process. From a comparison to the calculated sequence distributions of the monomers in the copolymers, we conclude that the major mechanism for the migration of the excitation energy involves interactions between nonnearest neighbors in the chain.

**Acknowledgment.** This work was supported by the Office of Basic Energy Sciences of the Department of Energy (T.K.) and by the Natural Sciences and Engineering Research Council of Canada (J.E.G.). This is

Document No. NDRL-2290 from the Notre Dame Radiation Laboratory.

## References and Notes

- (1) Amerik, Y.; Guillet, J. E. *Macromolecules* 1971, 4, 375.
- (2) Dan, E.; Guillet, J. E. *Macromolecules* 1973, 6, 230.
- (3) Kato, M.; Yoneshige, Y. *Makromol. Chem.* 1973, 164, 159.
- (4) Lukac, I.; Zavara, I.; Hrdlovic, P.; Manasek, Z. *Chem. Zvesti* 1972, 26, 404.
- (5) Roussel, R.; Galin, M.; Galin, J. C. *J. Macromol. Sci., Chem.* 1976, A10, 1485.
- (6) Roussel, R.; Galin, J. C. *Ibid.* 1977, A11, 347.
- (7) Kilp, T.; Houvenaghel-Defoort, B.; Panning, W.; Guillet, J. E. *Rev. Sci. Instrum.* 1976, 47, 1496.
- (8) Azumi, T.; McGlynn, S. P. *J. Chem. Phys.* 1962, 37, 2413.
- (9) Kiwi, J.; Schnabel, W. *Macromolecules* 1975, 8, 430.
- (10) Wagner, P. J.; Kelso, P. A.; Kemppainen, A. E.; Zepp, R. G. *J. Am. Chem. Soc.* 1972, 94, 7500.
- (11) Shultz, A. R. *J. Polym. Sci.* 1960, 47, 267.
- (12) Wagner, P. J.; McGrath, J. M. *J. Am. Chem. Soc.* 1972, 94, 3849.
- (13) Lewis, F. D.; Hillard, T. A. *J. Am. Chem. Soc.* 1972, 94, 3852.
- (14) Wissbrun, K. F. *J. Am. Chem. Soc.* 1959, 81, 58.
- (15) David, C.; Demarteau, W.; Geuskens, G. *Polymer* 1969, 10, 21.
- (16) Weber, G. "Fluorescence and Phosphorescence Analysis, Principles and Applications"; Hercules, D. M.; Ed.; Interscience: New York, 1966; Chapter 8.
- (17) Schneider, F. Z. *Naturforsch.*, A 1969, 24A, 863.
- (18) David, C.; Baeyens-Volant, D.; Geuskens, G. *Eur. Polym. J.* 1976, 12, 71.
- (19) David, C.; Putman-DeLavareille, N.; Geuskens, G. *Eur. Polym. J.* 1977, 13, 15.
- (20) Jablonski, A. *Acta Phys. Pol.* 1958, 17, 481.
- (21) Ore, A. *J. Chem. Phys.* 1959, 31, 442.
- (22) Weber, G. *Trans. Faraday Soc.* 1954, 50, 554.
- (23) Harwood, H. J.; Ritchey, W. M. *J. Polym. Sci., Part B* 1966, 2, 601.
- (24) Inokuti, M.; Hirayama, F. *J. Chem. Phys.* 1965, 43, 1978.
- (25) Adamezyk, A.; Phillips, D. *Trans. Faraday Soc.* 1974, 70, 537.
- (26) Dörr, F. C. *Angew. Chem., Int. Ed. Engl.* 1966, 5, 478.
- (27) Herzberg, G.; Teller, E. *Z. Phys. Chem., Abt. B* 1933, B21, 410.

## Ultradrawing at Room Temperature of High Molecular Weight Polyethylene

Masaru Matsuo<sup>†</sup> and R. St. John Manley\*

*Pulp and Paper Research Institute of Canada and Department of Chemistry, McGill University, Montreal, Quebec, Canada H3A 2A7. Received February 9, 1982*

**ABSTRACT:** Films of ultrahigh molecular weight ( $6 \times 10^6$ ) polyethylene were produced by gelation/crystallization from dilute solutions according to the method of Smith and Lemstra. Under ambient conditions the dried gel films could be readily stretched to the remarkably high draw ratio of 20. This interesting phenomenon is discussed in terms of the morphology of the dry gel film as studied by wide-angle X-ray diffraction, small-angle X-ray scattering, and small-angle light scattering techniques. The facile drawability is thought to be due to the extremely high molecular weight and the low concentration of the solutions; these ensure a suitable level of the entanglement mesh that effectively transmits the drawing force.

## Introduction

There is currently considerable interest in the deformation behavior of polyethylene, with the ultimate goal of the production of ultrahigh-modulus films and fibers.<sup>1</sup> The deformation of the polymer molecules has been achieved both in the liquid phase, for example, in hydrodynamically or stress-induced crystallization,<sup>2,3</sup> and in the solid state, such as in solid-state extrusion<sup>4,5</sup> or in drawing processes.<sup>6-11</sup> Invariably, the most pronounced molecular extension was attained for polyethylene at elevated temperatures, generally above about 60 °C.<sup>1-11</sup>

In the present paper we report the remarkably high drawability at room temperature, with maximum draw ratios up to 20, of ultrahigh molecular weight polyethylene films ( $M_w = 6 \times 10^6$ ) that were produced by gelation/crystallization from semidilute solutions according to the method of Smith and Lemstra.<sup>8-11</sup> This interesting phenomenon was investigated by small-angle X-ray scattering (SAXS), wide-angle X-ray diffraction (WAXD), small-angle light scattering, and optical microscopy.

## Experimental Section

A linear polyethylene with the very high molecular weight of  $6 \times 10^6$  (Hercules 1900/90209) was used. Solutions containing 0.5% by weight of the polymer in decalin were prepared by heating well-blended polymer/solvent mixtures at 165 °C for 5 min and subsequently at 158 °C for 55 min. The homogenized solution

was poured into an aluminum tray that was surrounded by ice water to form a gel. The decalin was allowed to evaporate from the gels at ambient conditions for 14 days. The nearly dried film, which had a thickness of about 150  $\mu\text{m}$ , was immersed in an excess of ethanol for 1 day and subsequently dried for 6 days to remove residual traces of decalin.

The dried polyethylene films were cut into strips of length 50 mm and width 12 mm. These specimens were elongated at room temperature with an Instron tensile tester at a crosshead speed of 10 mm/min, which appeared by trial and error to be the most suitable rate. Draw ratios were determined in the usual way by measuring the displacement of ink marks placed on the specimen prior to drawing.

The various films were analyzed by optical microscopy, wide- and small-angle X-ray scattering, and light scattering. X-ray patterns were obtained with Ni-filtered Cu K $\alpha$  radiation produced by a Philips generator that was operated at 40 mA and 40 kV. Light scattering patterns were recorded using a 15-mW He-Ne gas laser as a light source. Diffuse scattering was avoided by sandwiching the specimen between cover glasses, with silicone oil (refractive index 1.533) as an immersion fluid.

## Results and Discussion

Figure 1 presents a typical nominal stress/strain curve that was recorded at room temperature for the dried polyethylene gel film. This figure evidently shows that under ambient conditions the remarkably high draw ratio of  $\sim 20$  was attained for this ultrahigh molecular weight polyethylene. This value should be compared with the so-called "natural draw ratio" at room temperature of melt-crystallized polyethylene, which ranges from 4 to 10, depending on the molecular weight of the sample.<sup>13</sup> The

<sup>†</sup> On leave from Nara Women's University, Nara, Japan.